THE JOURNAL OF PHYSICAL CHEMISTRY B

Article

pubs.acs.org/JPCB

Crystal Polymorphism of Hexylammonium Chloride and Structural Properties of Its Mixtures with Water

Valentina Migliorati,*[,†] Paolo Ballirano,*[,‡] Lorenzo Gontrani,[†,§] and Ruggero Caminiti[†]

[†]Dipartimento di Chimica, Università di Roma "La Sapienza", Piazzale Aldo Moro 5, 00185 Roma, Italy

[‡]Dipartimento di Scienze della Terra, Università di Roma "La Sapienza", Piazzale Aldo Moro 5, 00185 Roma, Italy

[§]CNR - Istituto di Struttura della Materia, Area della Ricerca di Roma 2, Tor Vergata, Via del Fosso del Cavaliere 100, I-00133 Roma, Italy

ABSTRACT: The thermal stability of hexylammonium chloride (HeAC) has been investigated in situ real time by high-temperature X-ray powder diffraction. A phase transition from a low-temperature (LT) tetragonal to a high-temperature (HT) cubic polymorph has been detected at 473 K. A first sharp diffraction peak (FSDP) starts to grow at the same temperature and disappears at 493 K, just before melting starts to occur. The dependence of cell parameters from temperature has been quantified for the LT polymorph and shown to be very anisotropic. In particular, the tetragonal *a* parameter expands, while the *c* parameter contracts, and as a net result, the volume increases. The HT polymorph shows features reminiscent of that of plastic phases of molecular crystals and is characterized by a less efficient packing as compared to the LT polymorph as indicated by a volume expansion of ca. 11%. Moreover, the structural properties of HeAC/water mixtures, up to very high dilution, have been investigated by combining MD simulations and X-ray diffraction experiments. By using a Cl−water Lennard-Jones parameter previously refined for a similar system, a very good agreement between the theoretical and experimental diffraction patterns was obtained for all the studied systems. The Cl^- ions in the mixtures were found to form both a first and second shell of water molecules. Moreover, a complex structural behavior has been highlighted, in which a strong interaction between cations and anions survives also in conditions of very high dilution. As a consequence, cations and anions do not always possess a completely closed hydration shell of their own, but rather solvent-shared ion pairs are formed to some extent in all the investigated mixtures.

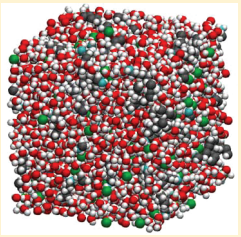

INTRODUCTION

Fluids composed solely of ions, such as molten salts and plasmas, show peculiar properties that are absent in liquids with neutral molecular components. These materials are characterized by slow decaying electrostatic interactions and have been extensively studied in the past from both an experimental[1] and theoretical[2] point of view.

Among the several families of molten salts, alkylammonium chlorides are particularly interesting due to the possibility of tailoring the volume and shape of the organic cation by introducing different hydrocarbon chains.[3] In particular, when the length of the alkyl chain attached to ammonium cation is changed, a wide variation in the physicochemical properties of these compounds, such as solubility, viscosity, and melting point, can be obtained.[3,4]

Alkylammonium chlorides have found wide application for example as reagents in organic and analytical chemistry and in electrochemistry as supporting electrolytes.[3] Nevertheless, a detailed knowledge, at a molecular level, of the interactions present in these materials is still missing, and it is clear that the spectrum of possible applications could be greatly amplified by a deep comprehension of their physicochemical behavior based on a more precise microscopic description of these materials. Among the various issues needing a more thorough understanding, there are the crystal polymorphism of solid alkylammonium chlorides and their behavior in mixture with other solvents such as water.[5,6]

We have therefore undertaken a broad investigation of this class of materials, and in recent works we have studied the crystal polymorphism of two of the shortest homologues of the family of monosubstituted alkylammonium chlorides, namely ethylammonium chloride (EAC) and propylammonium chloride (PAC).[5,6] In particular, the temperature dependence of EAC and PAC structure has been investigated by *in situ* laboratory parallel-beam X-ray powder diffraction and, for both samples, polymorphic transitions have been observed, at 358 and 403 K for EAC and PAC, respectively.[5,6]

The structural properties of EAC/water and PAC/water mixtures with similar water concentration have also been studied by combining X-ray diffraction measurements and classical molecular dynamics (MD) simulations.[5,6] By refining a single interaction potential for the EAC/water mixture[5] and then using the same parameter for the PAC/water one,[6] a very good agreement between the theoretical and experimental diffraction patterns was obtained for both systems. The structural properties of the EAC and PAC/water mixtures were found to be very similar, and a complex structural behavior has been highlighted, in which cations and anions do not possess a completely closed hydration shell of their own. Conversely, solvent-shared ion pairs are formed, in which one

Received: December 14, 2011
Revised: January 20, 2012
Published: January 24, 2012

dx.doi.org/10.1021/jp2120466 | *J. Phys. Chem. B* 2012, 116, 2104−2113

or more water molecules act as a bridge between the anion and the cations.[5,6] The combination of theoretical and experimental techniques has been found to be essential to gain reliable structural information on the alkylammonium chlorides/water mixtures and this is not surprising since the study of the structural and dynamic properties of disordered systems is a complex task, and it is very difficult to obtain accurate information when using a single method of investigation.

In the present paper, we have used the powerful combined approach previously adopted for EAC and PAC to study the thermal and structural properties of an alkylammonium chloride with a longer alkyl chain, namely the hexylammonium chloride $C_6H_{13}NH_3Cl$ (HeAC), and its behavior in mixtures with water. As concerns the dependence of HeAC structure from temperature, a differential scanning calorimetric study has shown that several solid-phase transformations occur for this compound in the temperature range from −150 °C to its melting point.[7] The RT structure of HeAC has been shown to be tetragonal,[8] space group $P4/nmm$ a = 4.979(1) Å, c = 19.548(6) Å.[9] The nitrogen atoms that hop between four symmetrically equivalent positions are located in cavities formed by five chlorine atoms. Each nitrogen atom participates in three hydrogen bonds to neighboring chlorine ions. As concerns the hydrocarbon part of the structure, the first carbon−carbon bond is aligned almost perfectly along the 4-fold axis, whereas the remaining carbon atoms show different degrees of disorder.[9]

Therefore, the aim of the present paper is twofold: first, to provide the crystallographic data required for a complete understanding of the structural modifications occurring during heating of HeAC from RT to the melting point; second, to study the structural properties of HeAC/water mixtures as a function of water concentration up to very high dilution, by combining fully atomistic MD simulations and high energy X-ray diffraction experiments. One interesting issue that will be addressed is whether the solvent-shared ion pairs that are formed in the EAC and PAC/water mixtures[5,6] exist also in the HeAC/water mixtures, and if when the concentration of water molecules present in the mixtures is increased, the solvent-shared ion pairs continue to survive. Moreover, we will evaluate the performances of the Lennard-Jones parameter for the Cl− water interaction previously optimized for EAC,[5] and we will assess if it is able to correctly describe the structural properties also of alkylammonium chlorides with longer alkyl chain such as HeAC and in conditions of water concentration very different from those used for the force field refinement.[5]

METHODS

High-Temperature X-ray Powder Diffraction (HT-XRPD) Measurements. A sketch of the HeAC molecule is shown in Figure 1. Powder of the title compound was loaded

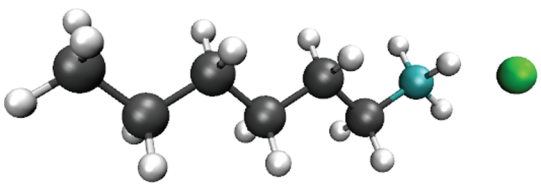

Figure 1. Sketch of the HeAC molecule.

and packed in a 1.0 mm diameter silica−glass capillary open at one end. The sample was used without any further purification. The capillary was glued to a 1.2 mm diameter Al_2O_3 tube by means of a high-purity alumina ceramic (Resbond 989). Diffraction data were collected on a parallel-beam Bruker AXS D8 Advance, operating in transmission in $\theta-\theta$ geometry. The instrument is fitted with a PSD VÅNTEC-1 detector set to a 6° 2θ aperture and with a prototype of capillary heating chamber.[10−14] Data were collected using Cu Kα radiation in the 3°−90° 2θ angular range, 0.0219° 2θ step size, and a counting time of 3 s. Isothermal measurements were carried out in the 303−523 K thermal range. A magnified view of the complete data set, consisting of 45 diffraction patterns, is shown in Figure 2.

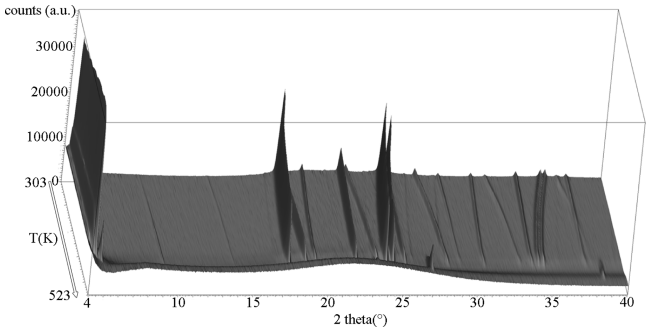

Figure 2. Magnified view (4°−40° 2θ) of the full data set of the heating run of HeAC.

X-ray Scattering Measurements. The X-ray scattering measurements were carried out for three HeAC/water mixtures with different water concentration. The HeAC/water molar ratios and the experimental densities of the investigated mixtures are reported in Table 1.

Table 1. Molar Ratios and Experimental Densities of the HeAC/Water Mixtures Investigated in This Work Together with the Sizes of the Corresponding Simulated Systems

HeAC/water molar ratio	exptl density (g/cm^3)	ion pairs	no. water molecules	simulation box edge (Å)
1:20.0	0.993	125	2500	47.05
1:49.0	1.00	64	3136	47.69
1:98.8	0.999	27	2668	44.15

In our previous works on EAC/water and PAC/water mixtures we used ion pairs/water molar ratio of 1:7.51 and 1:6.51, respectively. Here, it was not possible to reach such a high concentration of molten salt as the solubility of these compounds decreases with increasing length of the alkyl chain due to the higher degree of hydrophobicity. For this reason, the mixture with the highest concentration of molten salt that we have studied has a HeAC/water molar ratio of 1:20.0. Moreover, in order to study the structural properties of the mixtures as a function of water concentration, two additional mixtures up to very high dilution have been investigated.

HeAC was dried in vacuum for about 48 h. The HeAC/water mixtures were then prepared by adding a weighted amount of freshly distilled water to a weighted amount of solid HeAC in a round-bottomed flask. The samples were rapidly transferred into a cell sealed with Mylar windows. Sample and windows thicknesses were 3 mm and 6 μm, respectively. The large-angle X-ray scattering (LAXS) experiments were conducted using the noncommercial energy-scanning diffractometer[15,16] built in the

dx.doi.org/10.1021/jp2120466 | J. Phys. Chem. B 2012, 116, 2104−2113

Department of Chemistry, Rome University "La Sapienza". All of the details about the X-ray scattering measurements are described in refs 5 and 6.

The expression for the momentum transfer Q is

$$Q = \frac{4\pi \sin\theta}{\lambda} = 1.014E \sin\theta$$

where 2θ is the scattering angle, and E is expressed in keV and Q in Å^{-1}. The diffracted intensities recorded at the various angles were normalized to a stoichiometric unit of volume and merged to yield the total static structure factor $I(Q)$, which is given by

$$I(Q) = I_{eu}(Q) - \sum_{i=1}^{N} x_i f_i^2$$

where $I_{eu}(Q)$ is the observed diffracted intensity in electron units and x_i and f_i are the numerical concentrations of the atoms and their scattering factors. This function was multiplied by Q and by a Q-dependent sharpening factor, $M(Q)$:

$$M(Q) = \frac{f_N^2(0)}{f_N^2(Q)} e^{-0.01Q^2}$$

having chosen nitrogen as the sharpening atom. This procedure enhances the resolution of the curve at high Q values and decreases the truncation error in the calculation of the Fourier transform from reciprocal (Q) to direct space (r). The structure function $I(Q)$ has been Fourier-transformed into a radial distribution function ($D(r)$), according to the relation

$$D(r) = 4\pi r^2 \rho_0 + \frac{2r}{\pi} \int_0^{Q_{max}} QI(Q)M(Q) \sin(rQ)\, dQ$$

where ρ_0 is the system density and Q_{max} is the highest measured Q value (19.56 Å^{-1}).

If the uniform distribution component is dropped, which corresponds to the term $4\pi r^2\rho_0$, we obtain the differential correlation function Diff(r), which contains only the structural contribution to the distribution function.

Molecular Dynamics Simulation Details. The MD simulations of the HeAC/water mixtures were carried out using the DL_POLY package.[17] The HeAC/water molar ratios of the simulated systems were the same of those used in the experiments, and the number of ion pairs used in each simulation depended on the mixture and computational feasibility. The ions and the water molecules were placed in a cubic box, with periodic boundary conditions, and the size of the simulation box was chosen to reproduce the experimental density of the system under investigation. All of the parameters used in the simulations for the various systems are given in Table 1.

For the partial charges of the cation we have used the OPLS-AA charges for ammonium ions,[18] while all of the other force field parameters for the HeAC ion were taken from the Lopes and Padua force field.[19,20] For water one of the most widespread water models was employed, namely the TIP5P.[21] The TIP5P is a five-site model in which the oxygen is neutral, and the negative charge is placed on two massless dummy atoms located orthogonal to the water plane. In our recent works on mixtures with water of EAC and PAC, we have evaluated and compared the performances of the TIP5P with that of another popular water model, namely the SPC/E,[22] in providing a reliable description of the structural properties of alkylammonium/water mixtures and we have found that the results of the TIP5P simulations were in much better agreement with the experimental data, as compared to the SPC/E, thus showing that the TIP5P water model provided a better description of the structures formed in the mixtures.[5,6] The Lennard-Jones parameters for all of the unlike atoms were obtained from the Lorentz−Berthelot combining rules with the exception of one Lennard-Jones parameter for the Cl−water interaction ($\sigma_{Cl\text{-}OW}$), for which the value previously optimized for the EAC/water mixture was used.[5]

The MD simulation details were the same as those previously used in refs 5 and 6.

The theoretical structure factors $I(Q)$ were calculated from the MD simulations by using the equation[23]

$$I(Q) = \sum_{i=1}^{N} \sum_{j=1}^{N} x_i x_j f_i f_j H_{ij}(Q)$$

where H_{ij} are the partial structure factors, defined in terms of the radial distribution functions by the Fourier integral

$$H_{ij}(Q) = 4\pi\rho_0 \int_0^{r_{max}} r^2 (g_{ij}(r) - 1) \frac{\sin(Qr)}{Qr}\, dr$$

where ρ_0 is the bulk number density of the system and r_{max} is half the box edge.

The theoretical structure factors were calculated using in-house written codes. The theoretical $I(Q)$ was then multiplied by Q and by the same sharpening factor used for the experimental data, in order to obtain a theoretical $QI(Q)$ $M(Q)$ function that can be directly compared with the experimental data. The theoretical Diff(r) functions were also calculated as described before.

Angular distribution functions were calculated from the MD simulations for two different angles: the angle formed by two Cl−O vectors (labeled as ψ) and the angle formed by the Cl−O and O−H vectors (labeled as ω), where O and H are the oxygen and hydrogen atoms of the water molecules in the first hydration shell of the Cl^- ion. The angular analyses were carried out using in-house written codes as well.

RESULTS AND DISCUSSION

Crystal Polymorphism. A phase transition was observed at 473 K, whereas the melting process started at 498 K and was identified from an abrupt increase of the background counterbalanced by a strong general intensity reduction of the Bragg reflections. Such process reaches completion at 503 K.

RT data were initially evaluated by the Rietveld method using the model reported in ref 8 as starting structure. However, because of the reported structural disorder, the refinement provided no improvement with respect to reference data. Therefore, we only investigated the dependence of cell parameters and volume from temperature by LeBail fitting carried out with Topas 4.2.[24]

For the HT polymorph, 11 peaks were located by profile-fitting technique using Topas 4.2. Autoindexing was performed using TREOR90.[25] A solution was obtained in the cubic system for a cell parameter a = 6.5993(5) Å, volume = 287.44(1) Å^3, and the following figures-of-merit M_8 = 109 and F_8 = 31(0.0108,24).[26,27] The reported volume is consistent with Z = 1. A LeBail fitting carried out with Topas 4.2 pointed out to

dx.doi.org/10.1021/jp2120466 | J. Phys. Chem. B 2012, 116, 2104−2113

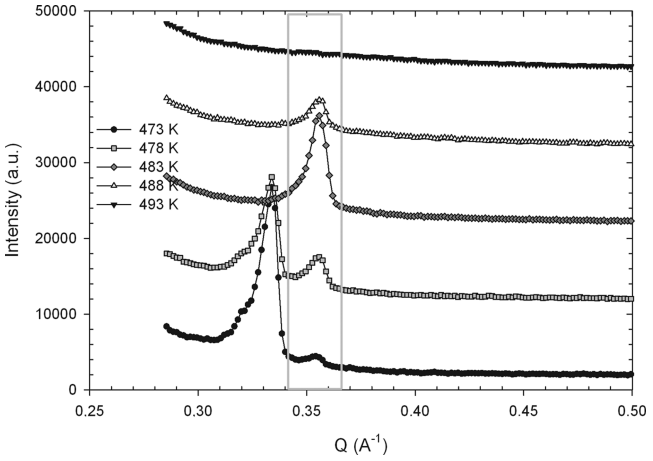

Figure 3. Evolution of FSDP, identified by the gray box, from 473 to 493 K. Diffraction patterns are vertically displaced for clarity.

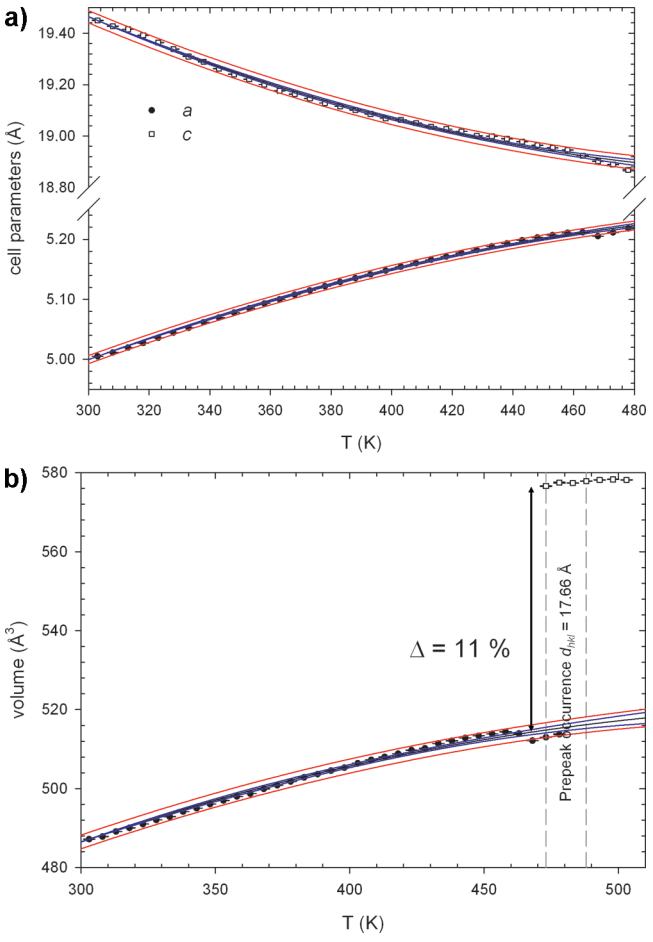

Figure 4. Evolution of cell parameters and volume with temperature: (a) cell parameters; (b) volume. Fitting of the expression $\alpha_V(T) = a_0 + a_1T$ (see below), confidence (95% level), and prediction intervals are also reported. Vertical dashed gray lines delimitate the thermal region in which FSDP occurs.

the reflection conditions *hkl* for $h + k = 2n$, $h + l = 2n$, $k + l = 2n$, 0*kl* for $k = 2n$, $l = 2n$, *hhl* for $h + l = 2n$, and 00*l* for $l = 2n$, consistent with the extinction symbol *F*---. After imposing such extinction conditions the figure of merit improved to $F_8 = 93(0.0108,8)$.

The phase transition starts to occur at 473 K and is completed at 478 K. In this thermal range both the LT and the HT polymorphs coexist. However, it is worth noting that at 473 K a new peak not related with the HT polymorph starts to grow in intensity. The calculated *d*-spacing is of ca. 17.7 Å, corresponding to *Q* ca. 0.35 Å^{-1}, a value slightly smaller than that of the relevant 100 reflection of the LT polymorph (Δ ca. 6.3%). Such peak reaches a maximum intensity at 483 K then starts to collapse until disappearance at 493 K (Figure 3).

This diffraction effect can be attributed to the so-called prepeak or first sharp diffraction peak (FSDP)[28] that has been detected in melted longer-chain alkylammonium chlorides. To the best of our knowledge, this is the first report of a FSDP under such conditions. Evolution of cell parameters and volume with temperature are reported in Figure 4.

According to the present results, thermal expansion is significantly anisotropic. In fact, the *a* parameter expands as a function of *T*, whereas the *c* parameter contracts. Within the investigated thermal range, the *a* parameter expands of 4.4%, whereas the *c* parameter contracts of 3.2% only. As a net result, the volume regularly increases. A jigsaw-shaped discontinuity on the quadratic dependence from temperature of the *a* parameter has been observed at $T > 463$ K. This irregularity may be due to precursory effects of the LT → HT phase transition. Therefore, significant differences are observed with respect to the recently described thermal behavior of both short-tailed EAC and PAC.[5,6] In fact, in the case of both EAC and PAC, linear thermal expansion is positive for all cell parameters. Besides, the volume thermal expansivity and the linear thermal expansion coefficients were calculated for the LT polymorph. All the cell-volume data were simultaneously fit to the equation $V(T) = V_{Tr} \exp[\int_{Tr}^{T} \alpha_V(T)\, dT]$, where V_{Tr} is the volume at reference temperature $T_r = 303$ K and α_V is a polynomial of the form $\alpha_V = a_0 + a_1T + a_2T^{-2}$.[29] Results of the fitting procedure, ignoring the T^{-2} term, are reported in Table 2.

Table 2. Linear and Volume Thermal Expansion Coefficients a_0 and a_1 of Low-Temperature HeAC[a]

		low-temp HeAC (303 K < *T* < 478 K)
a parameter	R^2	0.9977
	a_0 (×10^{-6})	361(4)
	a_1 (×10^{-8})	−65(3)
	a_{Tr}	5.00483(5)
c parameter	R^2	0.9952
	a_0 (×10^{-6})	−252(4)
	a_1 (×10^{-8})	52(3)
	c_{Tr}	19.4495(4)
V	R^2	0.9908
	a_0 (×10^{-6})	468(11)
	a_1 (×10^{-8})	−79(8)
	V_{Tr}	487.176(17)

[a]They were obtained by fitting the data to the expression $\alpha_V(T) = a_0 + a_1T$. a_{Tr}, c_{Tr}, and V_{Tr} are the *a* parameter, *c* parameter, and volume at reference temperature $T_r = 303$ K. R^2 = determination coefficients

As in the case of EAC,[5] at the transition temperature, the cell volume undergoes an expansion of ca. 11%. This indicates a less efficient packing of the HT polymorph. No attempt to determine the structure was performed because of its features reminiscent that of plastic phases of molecular crystals indicating the occurrence of significant rotational disorder of

dx.doi.org/10.1021/jp2120466 | J. Phys. Chem. B 2012, 116, 2104−2113

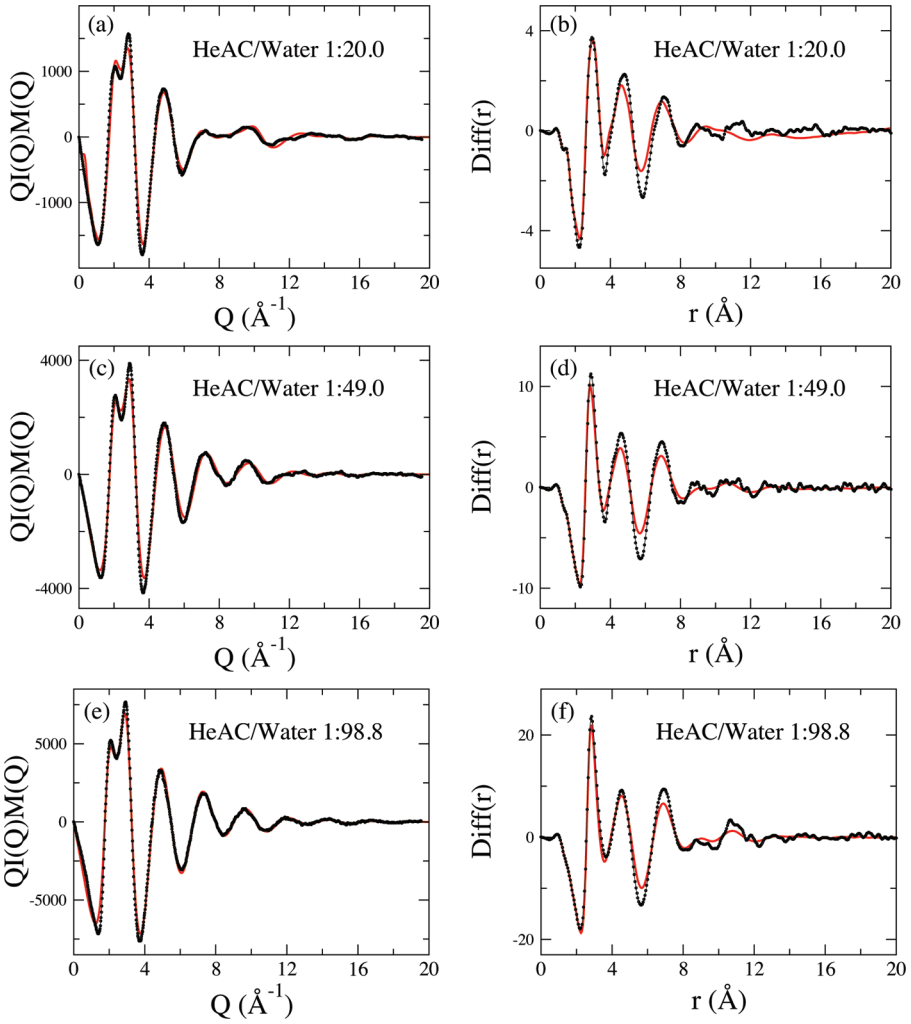

Figure 5. Comparison between the experimental structure factors (dotted black line) of the HeAC/water mixtures with ion pairs/water molar ratios of 1:20.0 (a), 1:49.0 (c), and 1:98.8 (e) and the theoretical structure factors (solid red line) calculated from the corresponding MD simulations. Comparison between the experimental Diff(r) functions (dotted black line) of the HeAC/water mixtures with ion pairs/water molar ratios of 1:20.0 (b), 1:49.0 (d), and 1:98.8 (f) and the theoretical Diff(r)'s (solid red line) calculated from the corresponding MD simulations.

the chain. A small expansion of the a-parameter of the HT polymorph with increasing temperature was observed.

Structural Properties of HeAC/Water Mixtures. The experimental X-ray diffraction patterns and Diff(r) functions of all the HeAC/water mixtures are shown as a dotted black line in Figure 5. As it can be seen, the experimental $I(Q)$'s show a very similar trend. In particular, they are characterized by a principal double peak, whose peak positions are found at about 2.07 and 2.88−2.92 Å^{-1}, followed by two less intense peaks centered at 4.83−4.85 and 7.22 Å^{-1}, and some less well-defined oscillations beyond. The Diff(r) functions of the three mixtures are also very similar to each other, being constituted by three main peaks, centered at about 2.95, 4.80, and 7.05 Å, at 2.90, 4.60, and 6.95 Å, and 2.85, 4.55, and 6.90 Å for the HeAC/water mixture with ion pairs/water molar ratio of 1:20.0, 1:49.0, and 1:98.8, respectively. Because of the strong anion−water interactions, to the large scattering factor of chlorine and to the large number of water molecules present in the mixtures, the main contributions to the first peak of the Diff(r) functions originate from contacts between the chloride ion and the oxygen atoms of water molecules belonging to the Cl^- first coordination sphere, and from oxygen−oxygen interactions between nearest-neighbor water molecules. The shift of the Diff(r) first peak toward shorter distances is due to the fact that the oxygen−oxygen contacts become more and more dominant with respect to the Cl−oxygen ones with increasing water content.

In order to interpret the X-ray diffraction data of the HeAC/water mixtures, we have carried out MD simulations of the three systems. As previously mentioned, in a recent work[5] we have investigated the structural properties of an EAC/water mixture by combining MD simulations and X-ray diffraction experiments, and with the aim of providing a reliable description of the system, we optimized a single force field parameter, namely the σ parameter of the Cl−OW Lennard-Jones potential, until the best possible agreement between the MD results and the experimental data was reached (we refer to the oxygen and hydrogen atoms of the water molecule as OW and HW, respectively). In a subsequent work,[6] we have carried out a combined MD and X-ray diffraction investigation of a PAC/water mixture, and by using the $\sigma_{Cl\text{-}OW}$ parameter previously refined for EAC, it has been possible to obtain a very good agreement between the theoretical and experimental diffraction patterns also of the PAC/water mixture. In order to assess if the same $\sigma_{Cl\text{-}OW}$ parameter is able to correctly describe the structural properties of the HeAC/water mixtures, we used

dx.doi.org/10.1021/jp2120466 | J. Phys. Chem. B 2012, 116, 2104−2113

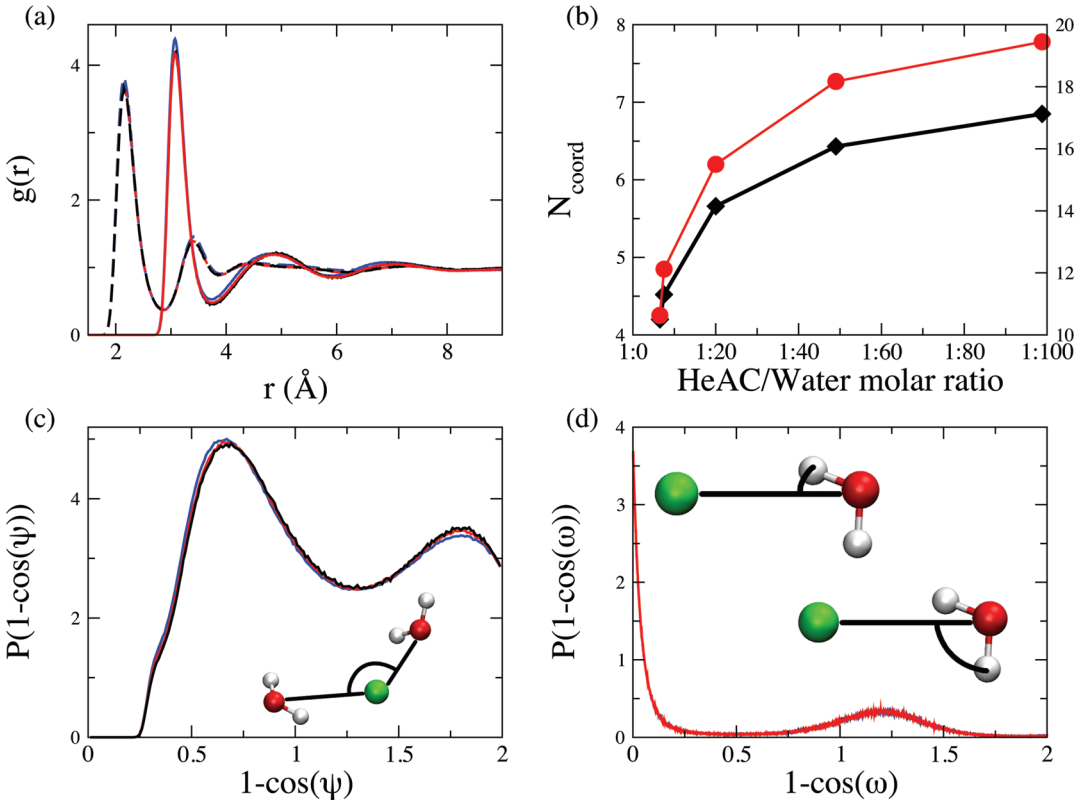

Figure 6. (a) Cl−OW (solid lines) and Cl−HW (dashed lines) radial distribution functions calculated from the MD simulations of the HeAC/water mixtures with ion pairs/water molar ratios of 1:20.0 (blue lines), 1:49.0 (red lines), and 1:98.8 (black lines). OW and HW are the oxygen and hydrogen atoms of the water molecules. (b) Coordination numbers of the water molecules in the first (black diamonds) and second (red circles) coordination shell of the Cl^- ion as a function of the HeAC/water molar ratio of the mixture. The scales are different on the left and the right axes, corresponding to the first-shell and second-shell coordination number, respectively. The first- and second-shell hydration numbers calculated from the MD simulations of EAC[5] and PAC[6]/water mixtures are also shown, corresponding to molar ratios of 1:7.51 and 1:6.51 for EAC and PAC, respectively. (c) OW−Cl−OW ψ angular distribution functions calculated from the MD simulations of the HeAC/water mixtures with ion pairs/water molar ratios of 1:20.0 (blue lines), 1:49.0 (red lines), and 1:98.8 (black lines). (d) ω angular distribution functions calculated from the MD simulations of the HeAC/water mixtures with ion pairs/water molar ratios of 1:20.0 (blue lines), 1:49.0 (red lines), and 1:98.8 (black lines).

the $\sigma_{Cl\text{-}OW}$ parameter previously optimized for EAC to treat the chloride−water interactions also in the present systems. As concerns the other interaction potentials, standard force field parameters reported in the literature have been employed as in previous studies[5,6] (see Methods section). The theoretical structure factors calculated from the MD simulations of the mixtures with HeAC/water molar ratio of 1:20.0, 1:49.0, and 1:98.8 are compared with the experimental ones in Figures 5a, 5c, and 5e, respectively. As it can be seen, the experimental pattern of peak positions and intensities is perfectly reproduced by the theoretical $I(Q)$'s in all the three systems. As far as the Diff(r) functions in distance space are concerned (Figures 5b, 5d, and 5f), also in this case a very good agreement between the theoretical and experimental Diff(r)'s was found for all the investigated mixtures.

It is noteworthy that such an excellent agreement between theory and experiment was obtained by using a $\sigma_{Cl\text{-}OW}$ parameter not specifically optimized for the present systems, indicating that the $\sigma_{Cl\text{-}OW}$ Lennard-Jones parameter optimized for EAC is transferable among the studied systems. Transferability of the functional form and parameters is an important feature of a force field as it means that the same set of parameters can be used to model a series of related molecules rather than having to define a new set of parameters for each individual molecule.

Once the validity of our MD simulations is assessed, insights into the structural properties of the HeAC/water mixtures can be obtained from the analysis of the trajectories. Structural arrangements of water molecules around the chloride ion are characterized by the Cl−OW and Cl−HW radial distribution functions, and the results obtained from the MD simulations are depicted in Figure 7a. First, it can be seen that the Cl-OW and Cl-HW are very similar in all the MD simulations of the mixtures with different HeAC/water molar ratios. The Cl-OW and Cl-HW $g(r)$'s calculated from the three simulations show very sharp and distinct first peaks, located at 3.07 and 2.15 Å for the oxygen and hydrogen atom, respectively. This result indicates that strong anion−water interactions are present, as previously observed for mixtures with water of the lower homologues of the alkylammonium chlorides family.[5,6] Moreover, in the Cl-HW $g(r)$'s two peaks are found, the former at shorter distances and the latter at longer distances as compared to the Cl-OW $g(r)$ first maxima, meaning that the first shell water molecules orient only one hydrogen atom toward Cl^-, as also shown for other halide ions in aqueous solution.[30] This is in line with the strong ability of the Cl^- ion to form hydrogen bonds. Another interesting feature that emerges from the Cl−water $g(r)$ analysis is the existence of a second solvation shell of water molecules around the Cl^- ion, as evidenced by a broad second peak of the Cl−OW $g(r)$, located between 3.76 and 5.90 Å, with a maximum at about 4.85 Å. Note that a second

dx.doi.org/10.1021/jp2120466 | J. Phys. Chem. B 2012, 116, 2104−2113

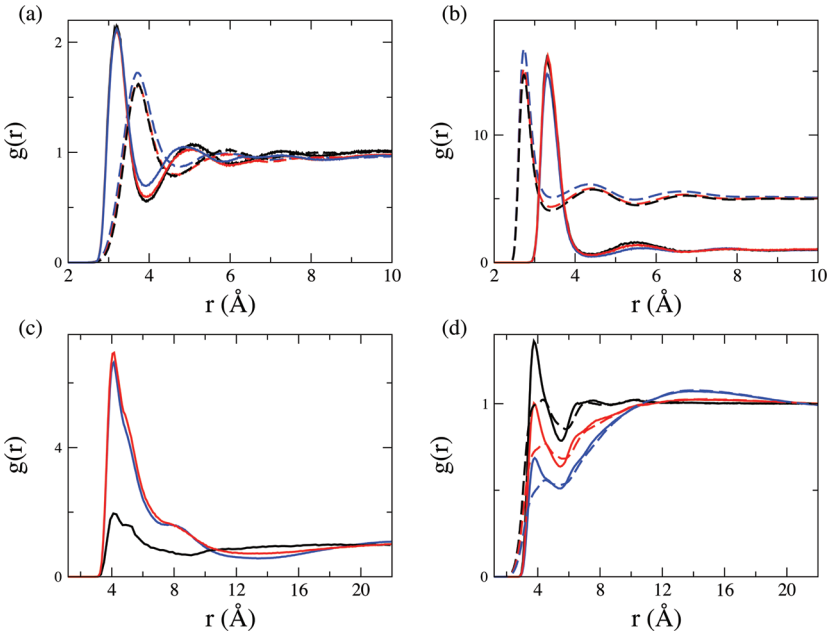

Figure 7. (a) N−OW (solid lines) and N−HW (dashed lines) radial distribution functions calculated from the MD simulations of the HeAC/water mixtures with ion pairs/water molar ratios of 1:20.0 (blue lines), 1:49.0 (red lines), and 1:98.8 (black lines). OW and HW are the oxygen and hydrogen atoms of the water molecules. (b) OW−OW (dashed lines) and Cl−N (solid lines) radial distribution functions calculated from the MD simulations of the HeAC/water mixtures with ion pairs/water molar ratios of 1:20.0 (blue lines), 1:49.0 (red lines), and 1:98.8 (black lines). The OW−OW $g(r)$'s are shown multiplied by a factor of 5 for clarity. (c) CT−CT radial distribution functions calculated from the MD simulations of the HeAC/water mixtures with ion pairs/water molar ratios of 1:20.0 (blue lines), 1:49.0 (red lines), and 1:98.8 (black lines). CT is the C atom of the terminal methyl group. (d) CT−OW (solid lines) and CT−HW (dashed lines) radial distribution functions calculated from the MD simulations of the HeAC/water mixtures with ion pairs/water molar ratios of 1:20.0 (blue lines), 1:49.0 (red lines), and 1:98.8 (black lines).

hydration shell was present also in the EAC and PAC/water mixtures previously investigated by our group, even if the intensity of the Cl−OW second peak was lower, as a consequence of the significantly lower water concentration used in those systems.[5,6]

To better exploit the structural properties of the Cl^- ion hydration shells, we have computed the coordination numbers of water molecules in the Cl^- first and second solvation spheres by integrating the Cl−OW $g(r)$ up to the first and second minimum, respectively. All the computed coordination numbers are shown in Figure 6b as a function of the HeAC/water molar ratio. The first- and second-shell hydration numbers calculated from the previously published MD simulations of EAC and PAC/water mixtures are also reported in Figure 6b, corresponding to alkylammonium chloride/water molar ratio of 1:7.51 and 1:6.51 for EAC and PAC, respectively. The cutoff values used in the calculation of the coordination numbers were the same for all the investigated mixtures, i.e., 3.76 and 5.90 Å for the first and second hydration shell, respectively. It comes out that with increasing water content the coordination numbers of water molecules in the Cl^- first and second coordination sphere increase accordingly. The slope of the increase is less steep for molar ratios of water molecules to ion pairs larger than about 1:40, as the water aggregation around anions approaches a saturation limit. As concerns the first hydration sphere, at the highest simulated water content, the first shell contains 6.9 water molecules. The coordination number of the Cl^- ion in aqueous solution as determined by X-ray and neutron diffraction studies is in the range 5−11, with a strong preference for 6,[31−35] while the results of MD and Monte Carlo simulations suggested a coordination number comprised between 5.6 and 8.4.[34,36−39] This scattering of the results present in the literature, which is characteristic also of other halide ions,[34] underlines the difficulty of defining the halide coordination shells also as a consequence of the fast water exchange between the first and second hydration spheres. However, the coordination number we found for the highest water concentration is well within the theoretical and experimental range predicted for the Cl^- aqua ion. As far as the second coordination shell is concerned, the number of water molecules that gather around the ion in the second sphere is between 2 and 3 times larger than the number of water molecules belonging to the first shell. This can be explained by the fact that only one hydrogen bond site of the possible four sites on each water molecule is involved in hydrogen bond with the anion, while the other sites are free to form up to three hydrogen bonds with second shell water molecules.

The geometrical arrangement of the first shell water molecules around the Cl^- ion can be evaluated by looking at the angular distribution functions of the O−Cl−O ψ angle, plotted in Figure 6c as $1 - \cos\psi$. The ψ distributions obtained from the three trajectories drop to zero for $1 - \cos\psi$ values lower than 0.25, showing that ψ angles smaller than 41° are prohibited in both simulations. Moreover, two broad peaks are found at $1 - \cos\psi = 0.65$ and $1 - \cos\psi = 1.80$ ($\psi = 70°$ and $\psi = 143°$, respectively), and the distributions are similar to the functions previously obtained from an MD simulation of the Br^- ion in aqueous solution.[30] Interestingly, the ψ distributions are very similar for all the three MD simulations, and this means that the water structure around the Cl^- ion is the same regardless of the water contents of the mixture. This can be explained by the fact that the first shell of the chloride ion tends to have always 7 first neighbors, either water molecules or N

dx.doi.org/10.1021/jp2120466 | J. Phys. Chem. B 2012, 116, 2104−2113

Table 3. Structural Parameters of the Radial Distribution Functions $g(r)$'s Depicted in Figure 6 Calculated from the MD Simulations of the HeAC/Water Mixtures with Different Ion Pairs/Water Molar Ratios[a]

	R (Å)			N			
	1:20.0	1:49.0	1:98.8	1:20.0	1:49.0	1:98.8	cutoff distance (Å)
N−OW	3.20	3.20	3.20	4.88	5.55	5.96	3.93
Cl−N	3.30	3.32	3.30	1.29	0.71	0.38	4.41
OW−OW	2.74	2.74	2.74	4.08	4.39	4.49	3.40
CT−CT	4.12	4.15	4.10	5.50	2.95	0.57	7.50
CT−OW	3.79	3.75	3.75	8.16	11.7	17.0	5.50

[a] R is the position of the $g(r)$ first peak, and N is the coordination number calculated by integration of the corresponding $g(r)$. The cutoff distances used in the calculation of N are also reported. Note that they were the same for all the investigated HeAC/water mixtures.

atoms of the cations (see the analysis of the instantaneous coordination numbers below).

The orientation of a single water molecule in the first hydration shell can be inferred from the distribution function of the ω angles (Figure 6d), which is the angle formed by the Cl−O and O−H vectors (O and H are the oxygen and hydrogen atoms of the water molecules belonging to the Cl^- first hydration shell). In all MD simulations the ω distributions are almost coincident and are consistent with a linear Cl---H−O hydrogen bond. Indeed, the sharp peak located at 0° indicates that one hydrogen atom of the first shell is strongly bound to the anion in a linear Cl---H−O configuration. The second hydrogen atom, which is less tightly bound and more free to rotate, is responsible for the second peak which is less intense and broader than the first one, whose maximum is found at 102°. These distributions are in agreement with previous calculations on anions in water.[30]

In order to gain an overall view of the structural properties of the HeAC/water mixtures, we have calculated the $g(r)$'s of a selected subset of atoms (see Figure 7), and selected first peak positions are reported in Table 3. We also computed a series of coordination numbers by the numerical integration of the radial distribution functions up to a certain cutoff. For each selected couple of atoms, the cutoff distance has been chosen as the position of the first minimum of the corresponding radial distribution function. The coordination numbers obtained from the trajectories are reported in Table 3, together with the cutoff values used in the calculations. The N−OW and N−HW $g(r)$'s calculated from the three MD simulations (Figure 7a) show the existence of a first hydration shell of water molecules around the N atom of the cation, but the peaks are less pronounced as compared to the Cl−water $g(r)$'s, as a consequence of weaker cation−water interactions as compared to the anion−water ones. The first shell water molecules on average prefer to orient the oxygen toward the N atom, but the oxygen and hydrogen $g(r)$ first peaks are not well separated and a larger orientational freedom is found, as compared to the chloride first hydration shell. With increasing water content the N−OW coordination number increases accordingly. Even if the water molecules strongly interact with Cl^- and with HeA, cations and anions are not completely separated, as shown by the strong Cl−N correlation that is found in all the simulations (Figure 7b). The Cl−N coordination number decreases as the water concentration increases, but it remains different from zero also for the most dilute solution. This is a first indication that "solvent-shared ion pairs" are present in HeAC/water mixtures and continue to survive also for very high concentration of water molecules. Moreover, the high and well-defined short-range peak of the OW−OW $g(r)$ (Figure 7b) suggests that the water molecules in the mixture tend to aggregate and form water clusters. The OW−OW coordination number is almost four, and it slightly increases with water content.

As far as the carbon atom of the terminal methyl group is concerned (CT), the presence of a peak at about 4 Å in the CT−CT $g(r)$ (Figure 7c) indicates that the cation alkyl chains aggregate to some extent in HeAC/water mixtures. The extent of tail−tail aggregation is strongly reduced by the increase of the ion pairs/water molar ratio, as evidenced by the strong decrease of CT−CT coordination numbers. Conversely, the CT atom becomes more and more hydrated with increasing dilution (Figure 7d), and the CT−OW coordination number significantly increases. For all the investigated mixtures, the positions of the CT−OW and CT−HW $g(r)$ first peaks are quite similar, thus suggesting an almost tangential arrangement of water molecules in the vicinity of the methyl group.

In the complex network of interactions that are built up in HeAC/water mixtures, a quantitative insight into the local environment seen by the Cl^- ion can be gained by defining an instantaneous coordination number n of Cl^- as the number of atoms of a certain type (X) at a distance from chloride shorter than the Cl−X $g(r)$ first minimum (see Table 3) and analyzing its variation along the simulations. In particular, we have calculated the coordination number distributions for the oxygen atom of the water molecules, for the N atom of the cations and for the sum of the oxygen and nitrogen atoms (see Figure 8). The results of this analysis show that in all the MD trajectories the Cl^- ion transits among several Cl−OW and Cl−N coordination numbers and the single distributions obtained for different molar ratios strongly depend on the water content of the mixture. Interestingly, this dependence is lost when the total coordination number is calculated Cl−(OW + N). If one considers the first shell complex of chloride constituted of either OW or N, a dominant percentage of Cl^- first coordination shell containing 7 first neighbors is found for all the three MD simulations. In other words, the chloride ion seems to prefer a heptacoordinated first shell configuration, independently on the nature of the first shell ligands. Another important result emerging from the instantaneous coordination number analysis is that a certain percentage of Cl^- local environments having N atoms within the cutoff distance is still present also for the most dilute solution. As already mentioned, in our previous investigations of EAC and PAC/water mixtures, we found that cations and anions did not possess a completely closed hydration shell of their own, but rather, solvent-shared ion pairs were formed, in which one or more water molecules belonging to the first solvation shell of the anion could act as a bridge and thus be shared with the N atom of the cation.[5,6] The present results indicate that this solvent shared ion pairs exist also in HeAC/water mixtures, and they are able to survive also in conditions of very high concentration of water molecules.

dx.doi.org/10.1021/jp2120466 | J. Phys. Chem. B 2012, 116, 2104−2113

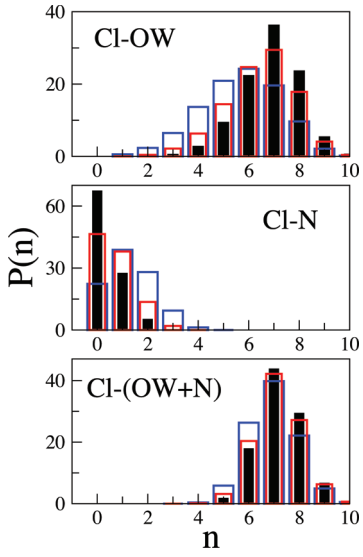

Figure 8. Distributions of the Cl^- instantaneous coordination number (n) calculated for the oxygen atom of the water molecules (Cl−OW), for the N atom of the cations (Cl−N), and for the sum of the oxygen and nitrogen atoms (Cl−(OW + N)). The results obtained from the MD simulations with HeAC/water molar ratio of 1:20.0, 1:49.0, and 1:98.8 are shown as empty blue bars, empty red bars, and full black bars, respectively.

More quantitatively, the percentage of these solvent shared ion pairs in each mixture corresponds to the percentage of nonzero Cl−N coordination numbers. As it can be seen, the ion pairs are the dominant configuration in the mixture with the lowest water concentration, and the percentage of solvent shared ion pairs decreases with increasing water content but remains nonzero also in very diluted solutions.

CONCLUSIONS

The investigation of the thermal stability of HeAC has disclosed the occurrence at 473 K of a phase transition from a LT tetragonal to a HT cubic polymorph. The HT polymorph occurs within the relatively narrow 473 K < T < 503 K thermal range. Both polymorphs coexists in the 473 K < T < 478 K thermal range. The HT polymorph shows features reminiscent of that of plastic phases of molecular crystals and is characterized by less efficient packing as compared to the LT polymorph as indicated by a volume expansion of ca. 11%. Within the 473 K < T < 488 K thermal range, before melting, a FSDP occurs. Its calculated d-spacing is of ca. 17.7 Å, corresponding to Q ca. 0.35 $Å^{-1}$, a value slightly smaller than that of the relevant 100 reflection of the LT polymorph. The evolution of cell parameters with temperature of the LT polymorph shows a peculiar behavior. In fact, the tetragonal a parameter expands, while the c parameter contracts, and as a net result, the volume increases. The cubic a parameter of the HT polymorph slightly expands.

Moreover, the structural properties of three HeAC/water mixtures with ion pairs/water molar ratios of 1:20.0, 1:49.0, and 1:98.8 have been investigated by combining MD simulations and X-ray diffraction experiments. The use of the $\sigma_{Cl\text{-}OW}$ Lennard-Jones parameter previously refined to obtain the best possible agreement between the MD structural results and the X-ray diffraction experimental data of an EAC/water mixture has allowed us to obtain here a very good agreement between the theoretical and experimental diffraction patterns for all the investigated mixtures. This is a very important result indicating that the $\sigma_{Cl\text{-}OW}$ Lennard-Jones parameter previously optimized is transferable between the studied systems, being able to correctly describe the structural properties of alkylammonium chlorides regardless of the length of the alkyl chain, even in conditions of water concentration very different from those used for force field refinement.[5]

From an accurate analysis of the MD simulations it turned out that the Cl^- ions in the mixtures form a first hydration shell of up to 7 water molecules that are bound to the anion with a nearly linear Cl---H−O hydrogen bond. Moreover, a second shell of water molecules around the anions was found containing between 2 and 3 times the number of water molecules belonging to the first hydration shell. The cation alkyl chains were found to aggregate to some extent in HeAC/water mixtures, and the tail−tail aggregation was strongly reduced with increasing dilution as the CT atom became more and more hydrated. A complex structural behavior has been highlighted in which both HeA^+ and Cl^- interact with water molecules, but the solvation of ions is not complete as a strong interaction between cations and anions is found in all the investigated mixtures, as evidenced by a sharp peak in the Cl−N $g(r)$. Insights into the local environment surrounding the Cl^- ion were obtained from the analysis of the instantaneous coordination number n of Cl^-: the chloride ion seems to prefer a heptacoordinated first shell configuration, constituted of either water molecules or HeA^+ cations interacting with Cl^- via the N atom. Altogether the present results show that cations and anions do not always possess a completely closed hydration shell of their own, but, rather, that solvent-shared ion pairs are formed to some extent. In particular, a dominant percentage of solvent shared ion pairs is found in the mixture with the lowest water concentration. This percentage decreases with increasing water content, but our results indicate that also in conditions of very high dilution the solvent shared ion pairs continue to survive.

AUTHOR INFORMATION

Corresponding Author

*E-mail: v.migliorati@caspur.it (V.M.); paolo.ballirano@uniroma1.it (P.B.).

Notes

The authors declare no competing financial interest.

ACKNOWLEDGMENTS

This work was supported by the University of Rome la Sapienza (Progetto Protic Ionic Liquids, ateneo 2010). Moreover it was supported by CASPUR with the Standard HPC Grant 2011 entitled “Protic ionic liquids”.

REFERENCES

(1) Bockris, J. O.; Reddy, A. K. N.; Gamboa-Aldeco, M. *Modern Electrochemistry: Ionics*; Plenum: New York, 1998.
(2) Hansen, J.-P.; McDonald, I. R. *The Theory of Simple Liquids*; Academic Press: New York, 1986.
(3) Zabinska, G.; Drozdowska, G.; Kisza, A.; Ferloni, P. *J. Chem. Eng. Data* **1998**, *43*, 562.
(4) Zabinska, G.; Urbaniak, G.; Kisza, A.; Ferloni, P. *J. Chem. Eng. Data* **1991**, *36*, 164.
(5) Migliorati, V.; Ballirano, P.; Gontrani, L.; Triolo, A.; Caminiti, R. *J. Phys. Chem. B* **2011**, *115*, 4887.
(6) Migliorati, V.; Ballirano, P.; Gontrani, L.; Russina, O.; Caminiti, R. *J. Phys. Chem. B* **2011**, *115*, 11805.

(7) Tsau, J.; Gilson, D. *J. Phys. Chem.* **1968**, *72*, 4082.
(8) Hendricks, S. B. *Z. Kristallogr.* **1928**, *68*, 189.
(9) Schenk, K. J.; Chapuis, G. *Z. Kristallogr.* **1983**, *162*, 197.
(10) Ballirano, P.; Maras, A.; Meloni, S.; Caminiti, R. *Eur. J. Miner.* **2001**, *13*, 985.
(11) Ballirano, P.; Melis, E. *Phys. Chem. Miner.* **2007**, *34*, 699.
(12) Ballirano, P.; Melis, E. *Phys. Chem. Miner.* **2009**, *36*, 319.
(13) Ballirano, P.; Sadun, C. *Struct. Chem.* **2009**, *20*, 815.
(14) Ballirano, P.; Caminiti, R. *J. Phys. Chem. A* **2009**, *113*, 7774.
(15) Caminiti, R.; Sadun, C.; Rossi, V.; Cilloco, F.; Felici, R. Italian Patent No. 01261484, 23 June 1993.
(16) (a) Carbone, M.; Caminiti, R.; Sadun, C. *J. Mater. Chem.* **1996**, *6*, 1709. (b) Abis, L.; Dell'Amico, D. B.; Busetto, C.; Calderazzo, F.; Caminiti, R.; Ciofi, C.; Garbassi, F.; Mascarelli, G. *J. Mater. Chem.* **1998**, *8*, 751.
(17) Smith, W.; Forester, T. *J. Mol. Graphics* **1996**, *14*, 136.
(18) Jorgensen, W. L.; Ulmschneider, J. P.; Tirado-Rives, J. *J. Phys. Chem. B* **2004**, *108*, 16264.
(19) Canongia Lopes, J. N.; Pádua, A. A. H. *J. Phys. Chem. B* **2004**, *108*, 16893.
(20) Canongia Lopes, J. N.; Deschamps, J.; Pádua, A. A. H. *J. Phys. Chem. B* **2004**, *108*, 2038.
(21) Mahoney, M. W.; Jorgensen, W. L. *J. Chem. Phys.* **2000**, *112*, 8910.
(22) Berendsen, H. J. C.; Grigera, J. R.; Straatsma, T. P. *J. Phys. Chem.* **1987**, *91*, 6269.
(23) Pings, C. J.; Waser, J. *J. Chem. Phys.* **1968**, *48*, 3016.
(24) Bruker AXS (2009) Topas V4.2: General profile and structure analysis software for powder diffraction data. Bruker AXS, Karlsruhe, Germany.
(25) Werner, P. E.; Eriksson, L.; Westdahl, M. *J. Appl. Crystallogr.* **1985**, *18*, 367.
(26) De Wolff, P. M. *J. Appl. Crystallogr.* **1968**, *1*, 108.
(27) Smith, G. S.; Snyder, R. L. *J. Appl. Crystallogr.* **1979**, *12*, 60.
(28) Annapureddy, H. V. R.; Kashyap, H. K.; De Biase, P. M.; Margulis, C. J. *J. Chem. Phys.* **2010**, *114*, 16838.
(29) Fei, Y. Thermal expansion. In *A Handbook of Physical Constants, Mineral Physics and Crystallography*; Ahrens, J. A., Ed.; AGU Reference Shelf 2, 1995; p 29.
(30) D'Angelo, P.; Migliorati, V.; Guidoni, L. *Inorg. Chem.* **2010**, *49*, 4224.
(31) Caminiti, R.; Licheri, G.; Piccaluga, G.; Pinna, G.; Radnai, T. *J. Chem. Phys.* **1979**, *71*, 2473.
(32) Caminiti, R.; Licheri, G.; Paschina, G.; Piccaluga, G.; Pinna, G. *Z. Naturforsch.* **1980**, *35a*, 1361.
(33) Caminiti, R.; Musinu, A.; Paschina, G.; Pinna, G. *J. Appl. Crystallogr.* **1982**, *15*, 482.
(34) Ohtaki, H.; Radnai, T. *Chem. Rev.* **1993**, *93*, 1157.
(35) Franks, F., Ed. In *Water. A Comprehensive Treatise*; Plenum Press: New York, 1979; Vol. *6*, Chapter 1.
(36) Clementi, E.; Barsotti, R. *Chem. Phys. Lett.* **1978**, *59*, 21.
(37) Mezei, M.; Beveridge, D. L. *J. Chem. Phys.* **1981**, *74*, 6902.
(38) Impey, R. W.; Madden, P. A.; McDonald, I. R. *J. Phys. Chem.* **1983**, *87*, 5071.
(39) Chandrasekhar, J.; Spellmeyer, D. C.; Jorgensen, W. L. *J. Am. Chem. Soc.* **1984**, *106*, 903.